

NUMERICAL MODELING OF SECONDARY FLOW IN MEANDERING ESTUARINE RIVER

GILLANG NOOR NUGRAHANING GUSTI

Civil and Environmental Engineering Department, Graduate School of Engineering, Hiroshima University, Higashihiroshima, Japan, m172908@hiroshima-u.ac.jp

KIYOSI KAWANISI

Civil and Environmental Engineering Department, Graduate School of Engineering, Hiroshima University, Higashihiroshima, Japan, kiyosi@hiroshima-u.ac.jp

ABSTRACT

The developed transversal flow in a river, known as secondary flow, is induced due to the instability of centrifugal forces along the vertical line of water body. In a saline environment, secondary flow undergoes further change by the presence of density stratification throughout the water body. Further, the existence of a structure such as sluice gate might further impose an alteration to the dynamics of secondary flow. The study here has been taken place on the Ota Diversion Channel in Hiroshima City, Japan that belongs in the Ota River system. This channel has its water flow blocked with a sluice gate in the upstream area. Here, a numerical model was used to investigate the transformation of secondary flow. Two scenarios were simulated by 10 σ -layers, the first scenario incorporates the existence of sluice gate and the second exempts it from the simulation. This study solely focused on the secondary flow during a spring tide period to eliminate the effect of increasing river discharge and spring to neap alteration. The numerical results show that the secondary flow is stronger with the existence of sluice gate rather than without it. The intrusion of saltwater could go further upstream without the existence of sluice gate thus generates a homogenous water body during high tide and ebb that dismisses the presence of stratification. Further evaluation of lateral momentum equation terms also manifest the transformation of baroclinic pressure gradient and centrifugal acceleration throughout the water body. These indicate that the presence of sluice gate indeed alters the structure of secondary flow in meandering estuarine river.

Keywords: Secondary Flow, Meandering Estuarine River, Estuary, Numerical Modeling, Sluice Gate

1. INTRODUCTION

A meanders-driven secondary flow is caused by the difference in centrifugal forces between the upper and lower layers of a curved flow (He, 2018). In the case of estuary, meanders modify the internal structure of the flows. The reduction in tidal current asymmetry in the meandering configuration may be attributed to two processes, reduction of flood currents but not of ebb currents seaward of the meanders and increased mixing of the ebb currents over a greater portion of the water column in the meandering region. Meanders also play an important role in redistributing material in the estuary, regardless of stratification, secondary flow is not shut down during stratified condition, but rather generates a more complex vertical structure including the baroclinically driven flow. On the other hand, stratification affects lateral circulation through mean and turbulent momentum terms. In both cases, stratification that occurs in the estuary would suppress the turbulence, thus the momentum budget must differ for stratified and well-mixed flows. Furthermore, the existence of tidal cycle induces variation over estuarine mixing as stratified water body arises during ebb and more homogenous during flood (Nidzieko et al., 2009).

The Ota River is a network of estuarine river branches that flow through Hiroshima City, Japan. the westernmost branch is called Ota Diversion Channel which separated from the upstream part of the Ota River network by a sluice gate (Gion Sluice Gate) that only allows ~10% of freshwater discharge under normal condition as shown in Figure 1 (Razaz et al., 2013). Hence, Ota Diversion Channel could be considered as semi closed estuarine river in which the existence of obstacle which blocks most of the freshwater discharge might further giving more complexity by altering the secondary flow structure. In this study the influences of sluice gate existence on the dynamics of secondary velocity is focused through hydrodynamic numerical simulation of Delft3D.

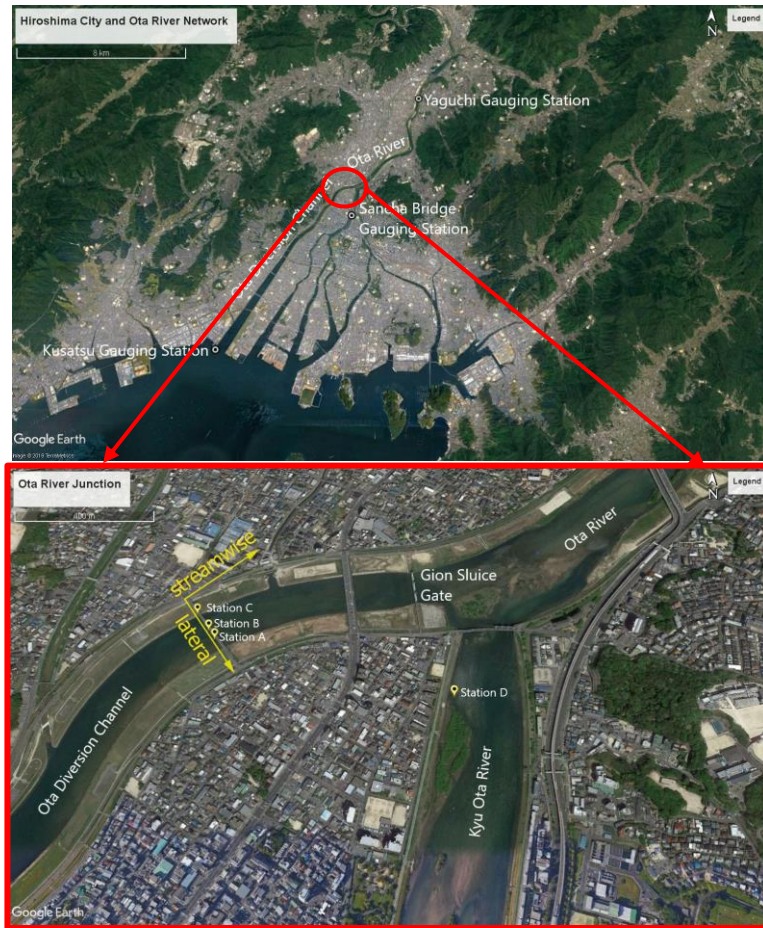


Figure 1. The Ota River network that flows through Hiroshima City (upper) and the detailed view of interest area where Gion Sluice Gate located (below). Yellow axes show the streamwise and lateral direction of the flow.

2. METHODS

2.1 Field measurement

A measurement program was conducted in the upstream section of Ota Diversion Channel near to the Gion Sluice Gate from November 23th 2018 until December 7th 2018. Three Acoustic Doppler Current Profilers (ADCPs) were installed on the bed along a transverse line (station A, B, and C) in the one of meanders in Ota Diversion Channel. These ADCPs were utilized to measure flow velocity and water level that are later used to validate results from numerical simulation. One Conductivity and Temperature (CT) Sensor and one Castaway CTD were also deployed in station A and D respectively to measure salinity for calibration and giving the boundary condition to the model (Station D). Bathymetry data was obtained through Coden Hydrographic Survey Remote Controlled Boat RC-S3 (Coden Co., 2012) along the Ota Diversion Channel and both Kyu Ota River and Ota River. Hourly water level was available from the the Ministry of Land, Infrastructure, Transport and Tourism (MLIT) of Japan water level gauges at Kusatsu (seaward end of Ota Diversion Channel) and Misasa Bridge (Kyu Ota River) Gauging Stations. Meanwhile, hourly river discharge was obtained through another MLIT gauge in Yaguchi Gauging Station.

2.2 Numerical simulation

Delft3D (Deltares, 2014) is a multidimensional hydrodynamic simulation program which able to simulate non-steady flow and transport phenomena resulting from interaction of tidal and metrological constraint acting on rectilinear or curvilinear boundary fitted grid (Deltares, 2014). It works based on the conservation of the mass and momentum of the incompressible fluid by applying hydrostatic assumption on the 3D RANS equations. Delft3D, which also employs quasi-3D model for its calculation, is proven to be able to simulate the secondary flow in meandering river according to Parsapour-Moghaddam and Rennie (2017). Moreover, assumption of hydrostatic pressure in Delft3D also proven to be able to simulate secondary flow (Nabi et al., 2016), despite it was simulated on 2D model. Considering the numerical advantages and its robustness to simulate hydrodynamics of tidal driven environment (especially estuaries), Delft3D adequately suited to simulate secondary flow dynamics in the Ota Diversion Channel.

In this model three open boundary were used for the convenient of interest area and availability. One was placed in the Ota River near the Yaguchi Gauging Station and specified by hourly series of river discharge and a constant salinity of 0 ppt. Two were placed close to Kusatsu Gauging Station near the sea and another one close to Misasa Bridge Gauging Station in the upstream area of Kyu Ota River, these two boundaries were specified by hourly series of water level and constant salinities of 25 ppt and 2 ppt respectively. As for the river system beyond the boundary of Kyu Ota river, it was not included as it is not counted as interest area of this study. The model was simulated for 24 days from November 14th until December 8th 2018

Here computational grid cells are set to correspond the bathymetry and riverbanks. Maximum number of grid cells for M and N direction (longitudinal and lateral, respectively) are 362 and 58 depending on the topography of river. The longitudinal resolution varies from 13m up to 65m. On the other hand, the lateral resolution is slightly less varied from the longitudinal with the highest resolution set at 7.5m and the lowest at 33m. Both orientations have higher resolution grid cells in the meandering area of Ota Diversion Channel. The influence of Gion Sluice Gate was taken into account by defining a sluice gate in the input of Delft3D that blocks 90% of the water flow. Two different scenarios, Scenario 1 (with sluice gate) and Scenario II (without sluice gate), were simulated to understand the effect of sluice gate existence on secondary flow. Figure 2 shows the computational grid cells while the overview of the parameter settings is given in Table 1.

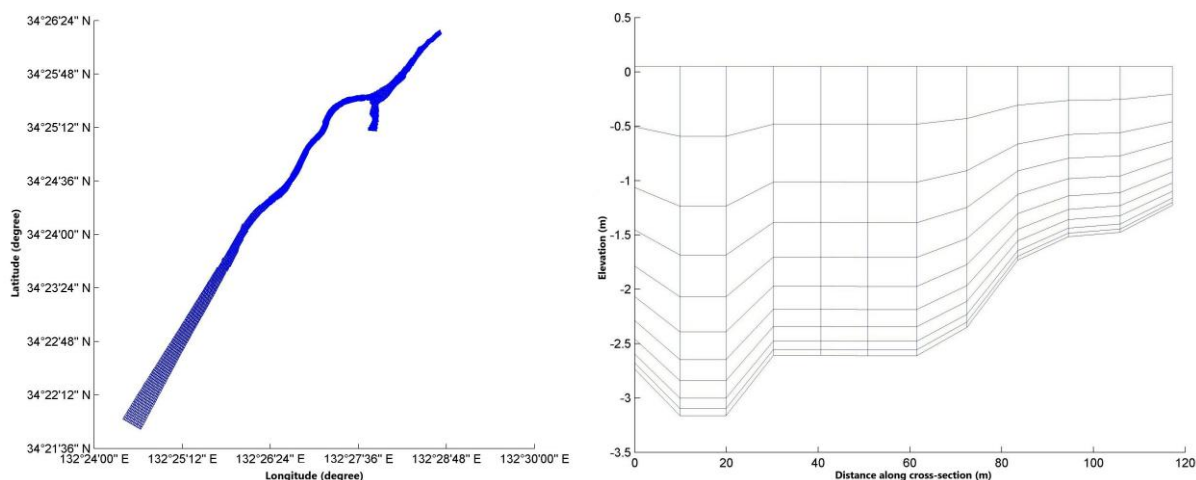


Figure 2. Top view (left) and cross-sectional view (right) of the computational grid cells.

Table 1. Parameter settings of the model

Variable	Settings
Number of layers	10 (σ -layers)
Simulation time	24 days
Time step	6 s
Local time zone	GMT +9
Initial water level	0.2 m
Initial salinity	14.7 ppt
Salinity value at Kusatsu boundary	25 ppt
Salinity value at Kyu Ota boundary	2 ppt
Salinity value at upstream boundary	0 ppt
Thatcher-Harleman time lag	0 min
Water density	1010.6 kg/m ³
Temperature	14.6 ⁰ C
Manning coefficient	0.035
Horizontal eddy viscosity	0.05 m ² /s
Horizontal eddy diffusivity	1 m ² /s
Vertical eddy viscosity	10 ⁻⁶ m ² /s
Vertical eddy diffusivity	10 ⁻⁶ m ² /s
3D turbulence model	<i>k-l</i>

2.3 Model evaluation

In order to evaluate the performance of numerical simulation, MAE: Mean Average Error, RMSE: Root Mean Square Error, and STD: Standard Deviation for water level, salinity, and flow velocity were calculated upon following equations:

$$MAE = \sum_{i=1}^n \frac{|a_{modi} - a_{obsi}|}{n} \quad (1)$$

$$RMSE = \sqrt{\sum_{i=1}^n \frac{(a_{modi} - a_{obsi})^2}{n}} \quad (2)$$

$$STD = \sqrt{\frac{\sum_{i=1}^n (|a_{modi} - a_{obsi}| - \mu)^2}{n - 1}} \quad (3)$$

a_{modi} and a_{obsi} are simulated parameter and observed parameter for i th time on certain location. μ indicates mean of all parameter error values and n is total observation time divided by 10 seconds as the interval time of data measurement.

3. RESULTS AND DISCUSSION

3.1 Model evaluation

Table 2 shows the calculated error statistics for the aforementioned parameters, MAE: Mean Average Error, RMSE: Root Mean Square Error, and STD: Standard Deviation. The value of error statistics of water level, east oriented flow velocity, and north oriented velocity were calculated before then averaged for station A, B, and C. Meanwhile, the value of error statistics for salinity was only calculated for station A. It has to be noticed that the error statistics calculations only applied to the scenario with sluice gate. During the observation period the sluice gate was never fully opened and thus the observation data for scenario without sluice gate could not be obtained.

Table 2. Calculated error statistics for simulation with gate

Parameters	MAE	RMSE	STD
Water level (m)	0.112	0.149	0.098
Salinity (ppt)	2.438	3.271	1.189
East oriented flow velocity (m/s)	0.077	0.086	0.039
North oriented flow velocity (m/s)	0.043	0.048	0.021

3.2 Secondary flow structure

To analyze the secondary flow structure, three-dimensional velocity flow fields were recorded in a meander located after Gion sluice Gate seaward-wise. A cross-sectional area, as shown in Figure 2, was chosen because it is near station A, B, and C where the model was evaluated. It has asymmetric bathymetry which resembles ordinary bathymetry of those found in meanders with shallow depth near the right bank and deeper depth in outer left bank. The lateral axis of the cross-section is defined to be positive to the southeast or to the direction of inner bank. The cross-section itself is observed from seaward direction.

During 24 days of simulation, the river discharge was low and fluctuating between $10 \text{ m}^3\text{s}^{-1}$ to $30 \text{ m}^3\text{s}^{-1}$ in the first twelve days. It then significantly increased with a peak discharge close to $68 \text{ m}^3\text{s}^{-1}$. The model also encountered two spring tides and one neap tide condition. To avoid the effects of increased river discharge and spring to neap variations, this study mainly focuses on the first spring tide event. The analysis here is done by the data taken during the high tide, low tide, flood and ebb for spring tide (November 25th 2018, twelfth day of simulation). Figure 3 shows the secondary flow and salinity structures for different tidal phases on scenario with sluice gate and without sluice gate consecutively.

In the scenario with sluice gate, it is shown that the secondary flow is stronger during the period of the active movement of water at flood and ebb than during the slack water when the water is supposed to have minimal movements. Figure 4 shows streamwise velocities for both scenarios during different tidal phases). In all tidal phases streamwise flow tends to be faster in the deeper outer part of the meander since the inner shallow part of meander might introduces high bottom friction that significantly reduce the flow. During the flood, the

secondary flow has similar pattern with ideal secondary flow in which the surface water moves to the direction of outer bank and the deeper water moves toward inner bank. This could be induced by partially mixed salinity along the cross-section that was formed during the flood. At ebb, which highly stratified, same secondary flow pattern was noticed although it is only for the outer part of the meander. Most of the cross-section area show three-layer circulation with the additional bottom layer directed toward the outer bank of the meander. This is similar with the stratified ebb condition that portrayed by in the previous study (Nidzieko et al., 2009). Although weaker than flood and ebb, secondary flow in stratified high tide and low tide have patterns that differ from them. During low tide, the pattern is a bit similar with the one during the ebb, but the outward secondary flow was weaker in the surface and its counterpart near the bottom has stronger flow. At the high tide, which is less stratified than the low tide, the patterns differ between each other on different locations. As shown in Figure 3, the middle and outer part of meander have similar pattern with those during the flood but the inner meander has opposite pattern with inward current in the surface and outward current near the bottom.

In the second scenario without sluice gate, the secondary flow is significantly weaker except at the low tide. During the low tide, most of the water body is occupied by fresher water than the saline water from the sea. Thus, it might induce such pattern of three-layer secondary flow that move inward in the surface, outward in the thick part of mid-depth, and thin inward directed layer near the bottom. Same pattern of secondary flow could be seen at flood for this scenario, even though it is weaker than the first scenario. The location of strong secondary flow also limited to be close to the cross-sectional halocline. As for both high tide and ebb, secondary flow were exceptionally weaker, if not even negligible, as the whole cross-section was fully mixed with salinity value as high as the Kusatsu Gauging Station, 25 ppt.

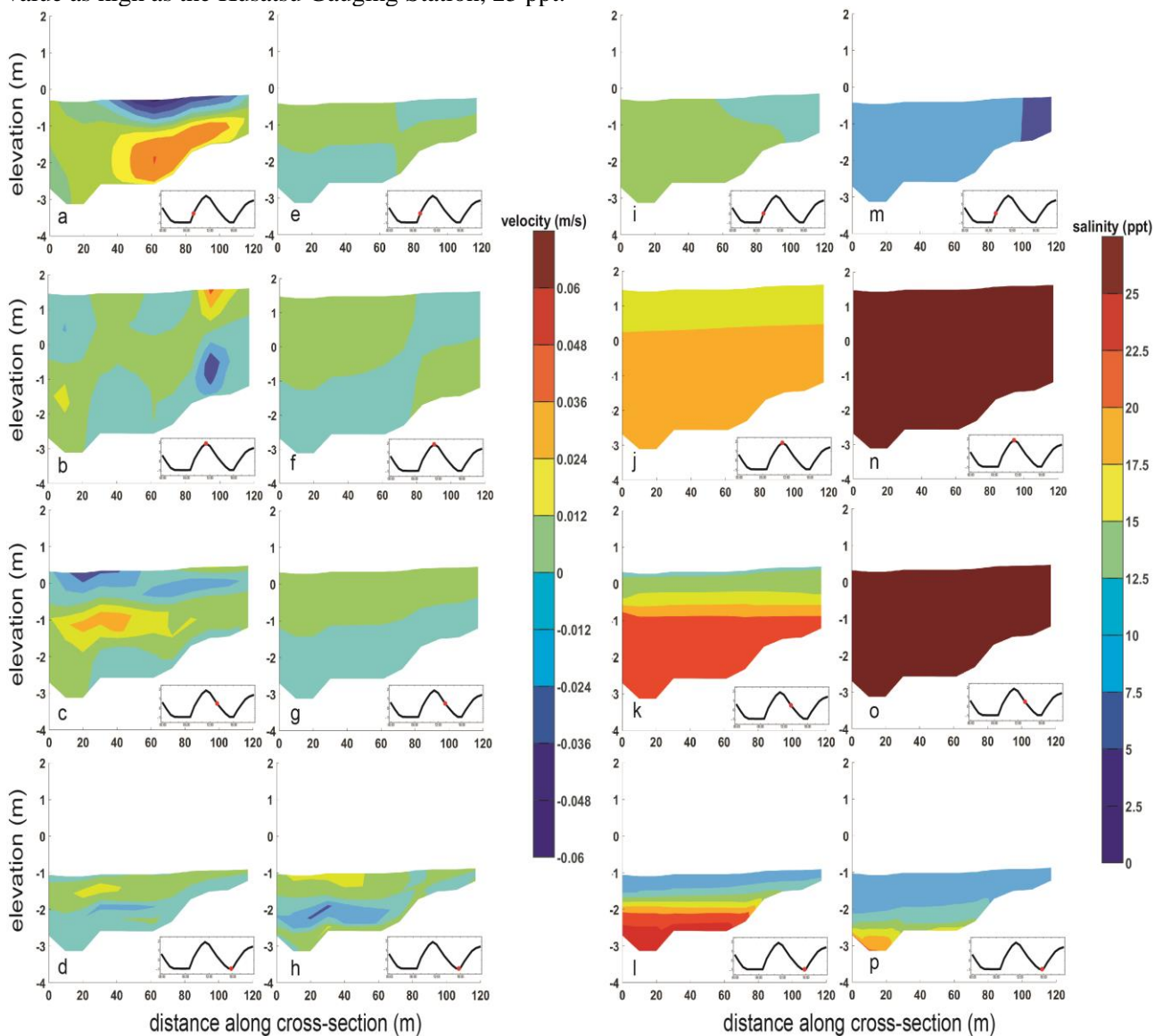


Figure 3. Secondary flow induced by tidal variation and sluice gate along the transversal line from outer bank to inner bank of meander (x- axis). Column 1 and 2 (from left) show the secondary velocity with the inclusion and exclusion of sluice gate respectively. Column 3 and 4 show salinity also with the inclusion and exclusion of sluice gate respectively. Row 1 is taken at flood. Row 2 represents high tide. Row 3 shows ebb. Row 4 is during low tide. The scale for secondary velocity ranges from -0.06 ms^{-1} to 0.06 ms^{-1} , positive values represent flow toward inner part of meander while the negative values show the opposite. Salinity ranges from 0 to 25. Small panels with black line depict the tidal phases.

The existence of sluice gate indeed affects the lateral structure of both salinity and secondary flow. Overall, the scenario with sluice gate set up secondary velocities that higher than those induced by the scenario without sluice gate. However, during the low tide secondary velocities of scenario without sluice gate was higher because the freshwater discharge was dominant over saltwater intrusion at that time. As the sluice gate was omitted in second scenario, Salinity in the cross-section reached its maximum value during both high tide and ebb (three hours before low tide) . This might mean that the Ota River is naturally an ebb-dominant estuary which able to intrude far to the upstream or to affect the Kyu Ota River from upstream direction. It is shown by the existence of maximum salinity even during the anterior half of ebb (Figure 3 o). The existence of sluice gate possibly limits this intrusion of saline water thereupon introduces stratification on the meanders of Ota Diversion Channel although river discharge from upstream become limited. Henceforth, the stratification strengthens vertical shear in the streamwise velocity that yields stronger secondary flow (Geyer, 1993).

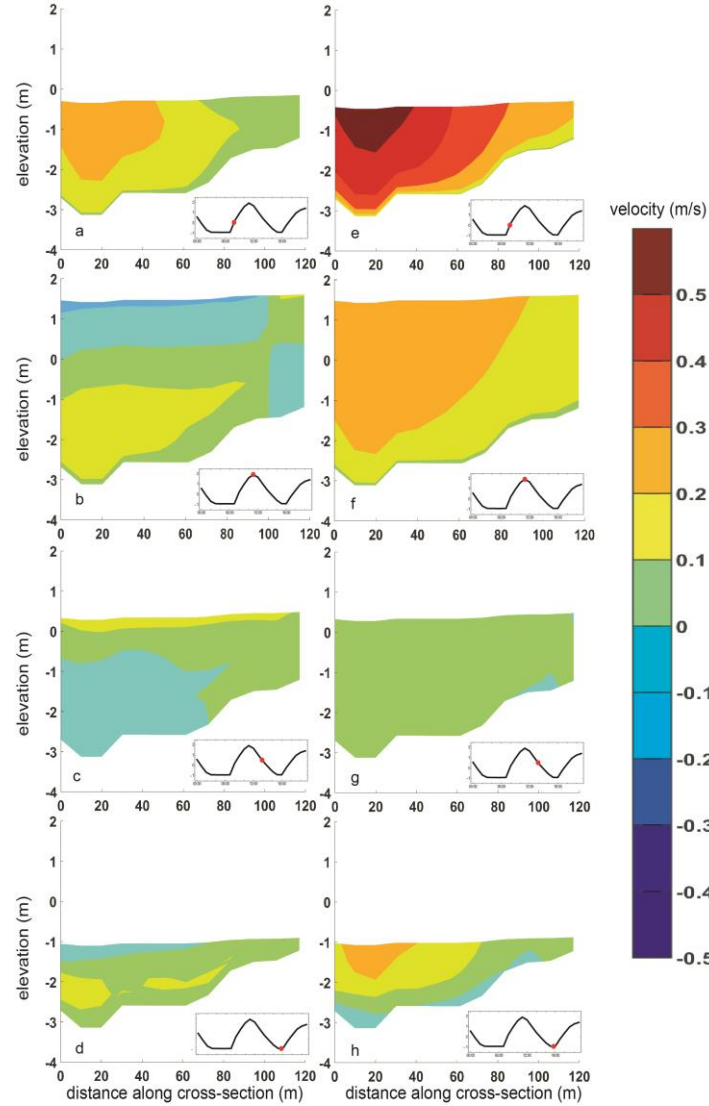


Figure 4. Streamwise velocity on different tidal phases at spring tide for Scenario I (left column) and Scenario II (right column). Row 1 is taken at flood. Row 2 represents high tide. Row 3 shows ebb. Row 4 is during low tide. The scale for streamwise velocity ranges from -0.5 ms^{-1} to 0.5 ms^{-1} with positive values show landward flow and negative values for seaward flow.

3.3 Governing mechanisms of secondary flow

In order to obtain more understanding about the governing mechanisms of secondary flow in Ota Diversion Channel, the lateral momentum balance is calculated. The lateral momentum equation is given by Equation (4).

$$\frac{\partial u_n}{\partial t} = -u_s \frac{\partial u_n}{\partial s} + \frac{u_s^2}{R_s} - g \frac{\partial \eta}{\partial n} - \frac{g}{\rho_0} \int_z^0 \frac{\partial \rho}{\partial n} dz - f u_s + \frac{\partial}{\partial z} \left(A_z \frac{\partial u_n}{\partial z} \right) \quad (4)$$

The n and s show lateral and streamwise direction, u_n and u_s represent the horizontal velocity in the lateral and streamwise direction respectively (for orientation-wise u_s was multiplied by -1 so that the seaward flow will be positive), R_s is the radius of curvature (this term will have negative value if the streamwise flow is landward), ρ_0 is constant reference density, ρ is the density of water, A_z indicates vertical eddy viscosity, and η denotes

surface water level. The terms within Equation (4) represent several forces that govern the pattern of secondary flow. The first term on the left-hand side is the time rate of change of secondary velocity at any vertical elevation of z . The first term on the right side represents nonlocal acceleration. The second term depicts centrifugal acceleration. The third term denotes barotropic pressure gradient. The fourth portrays baroclinic pressure gradient. The fifth term is Coriolis acceleration. The last term of Equation (4) is the turbulent shear stress in the stream-normal direction. Figure 5 shows the comparison of each term for different tidal phases, except for the Coriolis term as it is negligible on the scale of the estuary.

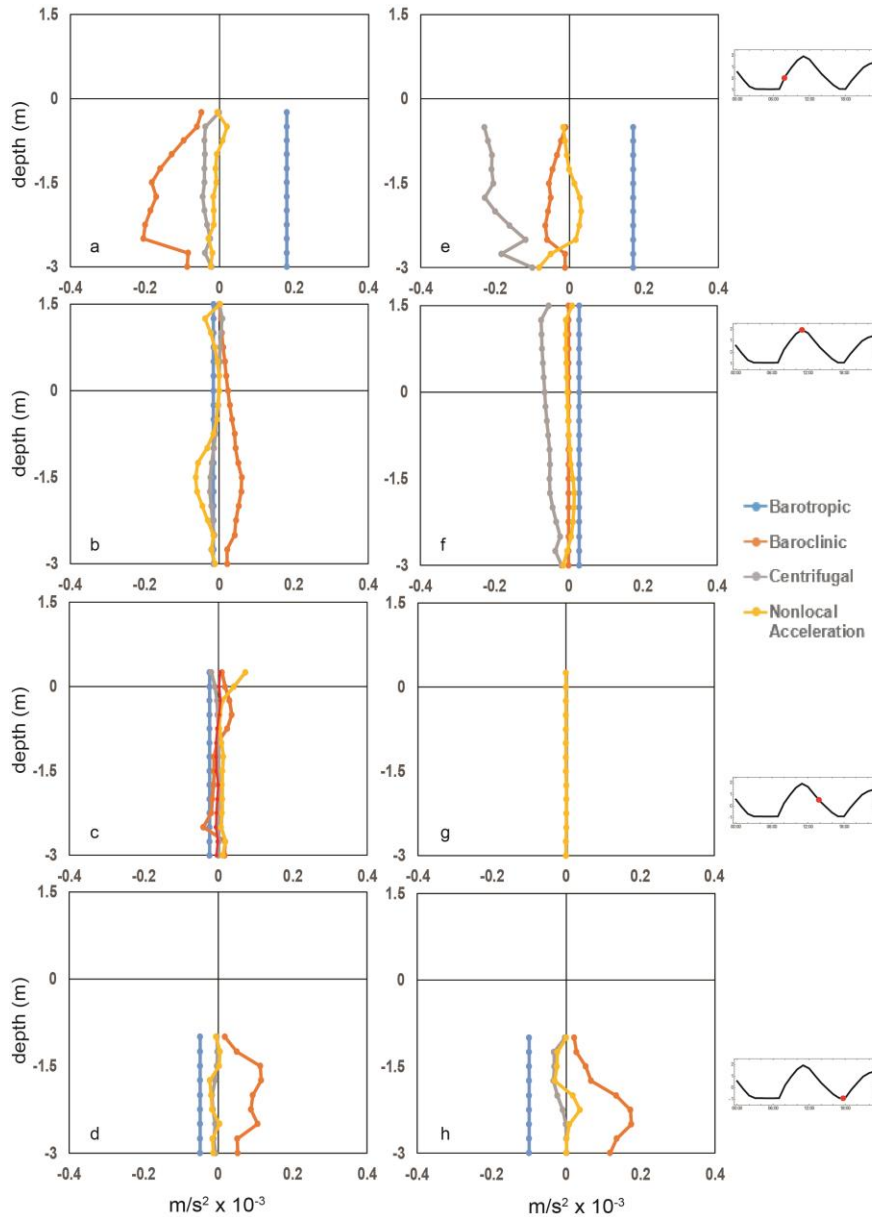


Figure 5. Governing Forces of secondary flow at spring tide for Scenario I (left column) and Scenario II (right column). Row 1 is taken at high tide. Row 2 represents ebb. Row 3 shows low tide. Row 4 is during flood. Positive values show positive gradient toward inner bank.

The assessment on momentum balance terms of secondary flow provides insight about the mechanisms that govern it in the meandering estuarine river with a sluice gate. The scenario with sluice gate in fact has greater baroclinic pressure gradient than the scenario without sluice gate except during low tide when freshwater discharge overcomes saltwater intrusion without any restrictions generated by sluice gate. On the other hand, the inexistence of sluice gate in the second scenario provides the water flow, either seaward or landward, to easily flow as it is proven by the higher value of centrifugal acceleration than the first scenario, especially during the flood. Overall, these two terms are mainly balanced by barotropic pressure gradient since the turbulent shear stress and nonlocal acceleration are found to be relatively insignificant.

4. CONCLUSIONS

The present work focused on the investigation of secondary flow in a meandering estuarine river that affected by a sluice gate through hydrodynamic numerical simulation. The simulation has been done for two scenarios

that distinguished by the existence of sluice gate. Nevertheless, a field observation has been done to give a vision into the evaluation of the simulation. After the simulation and analysis, it could be found that secondary flow is more intense on the scenario that includes sluice gate than the other scenario that exempts it. The existence of sluice gate produces two consequences on the flow in general. First, it blocks the 90 percent of the flow from both upstream and downstream which reduces streamwise flow thus the centrifugal acceleration term is minimized. Second, this blockage also introduces stronger stratification as the seawater that is supposed to be able to intrude further upstream was blocked. Hence, the baroclinic pressure gradient is greater in the scenario with sluice gate than the other scenario. These lead to a conclusion that sluice gate virtually alters the structure of secondary flow by shifting the centrifugal acceleration and baroclinic pressure gradient that govern the dynamics of secondary flow.

ACKNOWLEDGMENTS

This work was supported by Japan Society for the Promotion of Science (JSPS) KAKENHI grant number JP17H03313. The authors would also like to thank the members of Coastal Engineering Laboratory of Hiroshima University for their assistance

REFERENCES

- Coden Co. (2012). Coden Hydrographic Survey Operation Manual. Coden Co.
- Deltares. (2014). DELFT3D-FLOW hydro-morphodynamics user manual. Deltares.
- Geyer, W.R. (1993). Three-dimensional tidal flow around headlands. *Journal of Geophysical Research*, 98: 955-966.
- He, L. (2018). Distribution of primary and secondary currents in sine-generated bends. *Water SA*, 44: 118-129.
- Nabi, M., Ottevanger W., and Giri S. (2017). Computational modelling of secondary flow on unstructured grids. *Conf: ISRS 2016*. Taylor & Francis Group, London, pp. 719 – 726.
- Nidzieko, N.J., Hench J.L., and Monismith S.G. (2009). Lateral circulation in well-mixed and stratified estuarine flows with curvature. *American Meteorological Society*, 39: 831-851.
- Parsapour-Moghaddam, P. and Rennie C.D. (2017). Hydrostatic versus nonhydrostatic hydrodynamic modelling of secondary flow in a tortuously meandering river: Application of Delft3D. *River Res Applic.*, 33: 1400-1410.
- Razaz, M., Kawanisi K., Nistor I., and Sharifi S. (2013). An acoustic travel time method for continuous velocity monitoring in shallow tidal streams. *Water Resources Research*, 49: 1-15.